energies

MDPI

Article

Fast Pyrolysis of Municipal Green Waste in an Auger Reactor: Effects of Residence Time and Particle Size on the Yield and Characteristics of Produced Oil

M. M. Hasan [1,*], M. G. Rasul [1], M. I. Jahirul [1] and M. M. K. Khan [1,2]

[1] Fuel and Energy Research Group, School of Engineering and Technology, Central Queensland University, Rockhampton, QLD 4701, Australia; m.rasul@cqu.edu.au (M.G.R.); m.j.islam@cqu.edu.au (M.I.J.); masud.khan@aut.ac.nz (M.M.K.K.)

[2] School of Engineering, Computer and Mathematical Sciences, Auckland University of Technology, Auckland 1010, New Zealand

* Correspondence: m.m.hasan@cqu.edu.au

Abstract: The development of renewable sources for energy production has assumed a vital role in recent years, particularly with regard to the preservation of energy supplies and the environment. In this regard, municipal green waste (MGW) can be a potential renewable energy source if it is integrated with emerging technology, like pyrolysis. Therefore, this study aimed at investigating the effect of residence time and particle size on the yield and composition of oil derived from MGW using fast pyrolysis in an auger reactor. The residence time and particle size were varied from 1 min to 4 min and 1 mm to 10 mm, respectively, while keeping the temperature constant at 500 °C. At a residence time of 3 min, a 2 mm particle size provided the highest bio-oil yield (39.86%). At this experimental setting, biochar yield of 27.16% and syngas yield of 32.98% were obtained. The characterization of produced bio-oil revealed that a total of nine functional groups were present in the bio-oil. The phenols were highest in amount, followed by aromatics and ketones. The increase in residence time decreased the amount of acidic compounds present in the bio-oil. The water content was decreased by ~11% and the calorific value was increased by ~6% with the increase in particle size from 1 mm to 10 mm. Other properties, such as viscosity, density, cetane number, and flash point, did not change significantly with the change in experimental conditions. With a calorific value of 25+ MJ/kg, although the bio-oil produced from MGW can be used for heating (such as in boilers and furnaces), the use of MGW bio-oil in engines requires appropriate upgrading through procedures like hydrodeoxygenation, catalytic cracking, esterification, etc.

Keywords: municipal green waste; environmental degradation; waste to energy; fast pyrolysis; bio-oil; physicochemical properties

Citation: Hasan, M.M.; Rasul, M.G.; Jahirul, M.I.; Khan, M.M.K. Fast Pyrolysis of Municipal Green Waste in an Auger Reactor: Effects of Residence Time and Particle Size on the Yield and Characteristics of Produced Oil. *Energies* **2024**, *17*, 2914. https://doi.org/10.3390/en17122914

Academic Editor: Marcin Dębowski

Received: 8 April 2024
Revised: 8 June 2024
Accepted: 11 June 2024
Published: 13 June 2024

1. Introduction

The global issue of waste generation poses significant environmental risks resulting from various human activities. Current waste management systems are inadequate, posing threats to both the environment and human health [1]. Similarly, energy consumption, predominantly reliant on fossil fuels, contributes to environmental degradation. However, with fossil fuel reserves dwindling, alternative renewable energy sources are being sought to mitigate this issue [2–4]. Municipal green waste (MGW) holds promise as a renewable energy source. MGW refers to organic waste collected from urban areas. This type of waste typically includes biodegradable materials, such as grass clippings, leaves, branches and twigs, garden and yard debris, and plant trimmings. MGW is often gathered through community collection programs, and it is distinct from other types of municipal waste, such as household garbage, recyclables, or hazardous materials. However, with urbanization driving an increase in MGW production, effective management is crucial. While some

MGW can be utilized for gardening, excess must be managed efficiently to avoid risks and expenses. Thermal energy production from MGW shows potential, with technology playing a key role in optimizing its conversion into usable energy products.

Pyrolysis, an innovative technology, transforms MGW into diverse energy products like fuels and chemicals [5]. This process involves thermally decomposing carbon-rich materials without air, yielding bio-oil, biochar, and syngas. Unlike other methods, such as incineration or gasification, pyrolysis notably generates a higher volume of liquid energy product, particularly bio-oil, which is easy and safe to store and transport [6]. Bio-oil can serve as fuel in various applications, like boilers and furnaces. Among pyrolysis variations, fast pyrolysis stands out for its capacity to produce the most bio-oil, thus attracting significant research interest [7]. Choosing the right reactor and operating parameters is crucial for successful fast pyrolysis, as they greatly influence the quantity and quality of the resulting products [8]. Auger-type reactors are favored for their ease of handling and smooth operation, making them a practical choice for fast pyrolysis of MGW [9]. Hence, in the current study, an auger reactor was selected for conducting fast pyrolysis of MGW.

In fast pyrolysis, residence time and feedstock particle size are critical parameters influencing product yields. Longer residence times reduce bio-oil yield but increase syngas yield, as longer exposure to heat allows more volatiles to further decompose into non-condensable gases rather than condensing into liquids, whereas shorter residence times lead to incomplete pyrolysis, resulting in higher biochar yield [6,10]. Larger particle sizes typically increase heat transfer resistance, lowering actual temperatures within the feedstock and thus yielding less bio-oil but more biochar [11]. However, some studies have shown contradictory results. Consequently, there is no universal optimal residence time or particle size, as they vary depending on factors like feedstock and reactor type. Thus, having flexibility in choosing appropriate residence times and particle sizes for specific conditions can save time and money in fast pyrolysis processes. Hence, conducting experimental investigations to understand the effects of these variables on product yields and composition is crucial.

Numerous researchers [12–19] have carried out investigations on the effect of residence time and particle size on the yields and composition of pyrolysis products using MGW and other similar feedstocks. Sohaib et al. [12] performed experiments to investigate the effect of residence time on products obtained from fast pyrolysis of MGW in a semi-batch reactor. They observed that increasing the residence time from 10 s (seconds) to 30 s increased the bio-oil yield from 50.3% to 54.6%, respectively. A high-temperature slow pyrolysis of green waste collected from pine trunks was carried out by Solar et al. [13] in a continuous screw reactor. They found that the liquid pyrolysis product mainly contained water and some aromatic compounds. The evaluation of the effect of MGW particle size on the pyrolysis products was performed by Luo et al. [16]. Particle sizes ranging from 5 mm to 20 mm and a fixed bed reactor were utilized in their investigation. Their findings revealed that a decrease in particle size led to an increase in syngas yield, together with a reduction in the amount of bio-oil and biochar produced, as well as an increase in ash and carbon contents in the biochar. Similarly, Bennadji et al. [19] investigated the effect of particle size on bio-oil yield using waste wood as feedstock. They observed a strong influence of particle size on the devolatilization of feedstock during pyrolysis and yields of various chemical compounds of bio-oil.

Additional studies have further explored these effects. Zhang et al. [20] examined the impact of residence time on the quality and composition of bio-oil produced from corncob. They found that longer residence times favored the formation of phenolic compounds. Singh et al. [21] investigated the pyrolysis of agricultural residue and noted that varying residence times significantly affected the distribution of bio-oil, biochar, and syngas, with shorter times increasing bio-oil yields. Xiong et al. [22] studied the influence of particle size on the pyrolysis of pine sawdust, concluding that smaller particles enhanced the yield of bio-oil but also increased the production of undesirable tar compounds. Lastly, Charis et al. [23] conducted pyrolysis experiments on *Acacia tortilis* and pine dust. They

discovered that optimizing particle size could improve bio-oil quality while minimizing ash content. These studies collectively underscore the importance of selecting appropriate residence times and particle sizes to maximize the efficiency and quality of pyrolysis processes for different types of feedstocks.

It is clear from the published literature that the type of reactor and operating parameters, such as residence time and particle size, play a strong role in obtaining high yields of pyrolysis products. However, the combination of an auger reactor and fast pyrolysis to specifically investigate the effects of residence time and particle size on the yields and composition of bio-oil derived from MGW is not well-documented. Our study aims to fill this gap by applying a fast pyrolysis process in an auger reactor and conducting a detailed analysis of the chemical and physical properties of the produced bio-oils using Fourier Transform Infrared Spectroscopy (FTIR), Gas Chromatography–Mass Spectrometry (GC-MS), and physicochemical properties analysis. This approach not only maximizes the bio-oil yield but also provides new insights into optimizing the process for better-quality bio-oil production.

2. Materials and Methods

2.1. Feedstock and Sample Preparation

The MGW was obtained at the Waste Transfer Station in Rockhampton, Queensland, Australia in accordance with the American Society for Testing and Materials (ASTM) standard E 871-82 [24]. This standard requires a minimum collection amount of 10 kg. A total of 40 kg of mixed MGW was collected for this investigation, comprising hedge clippings, branches, tree trunks, stumps, as well as some soil and contaminants, which required extensive cleaning. Following the cleaning process, the MGW was exposed to direct sunlight for a period of 12 days in order to decrease its moisture content. Subsequently, the material was shredded into several dimensions (1 mm, 2 mm, 6 mm, and 10 mm) via a shredding device and afterwards subjected to sun-drying once more. Prior to introducing them into the reactor, the shredded materials were thoroughly mixed to achieve consistency. Figure 1 illustrates the collected and shredded MGW.

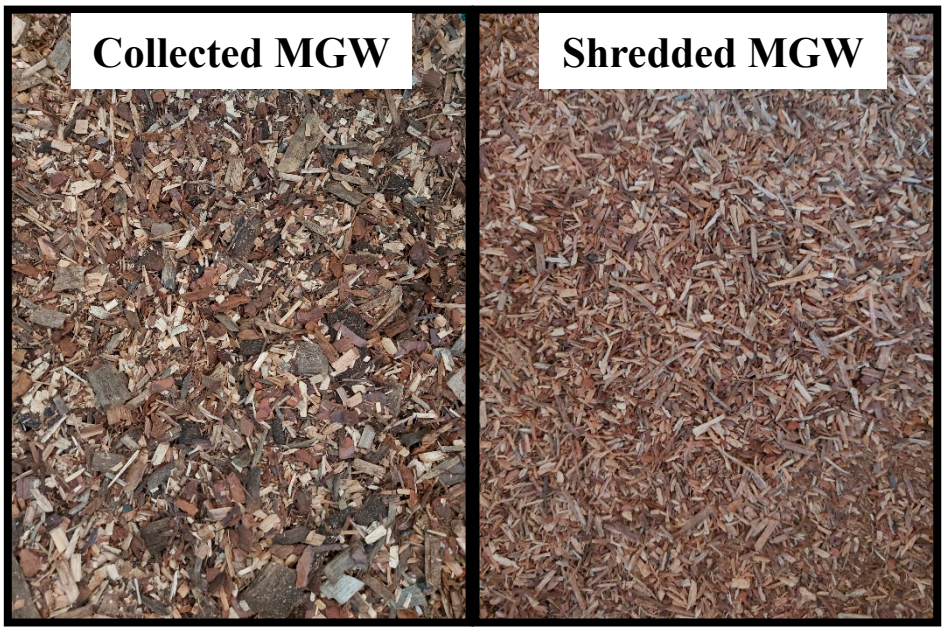

Figure 1. Photographs of collected and shredded MGW.

2.2. Experimental Setup

The fast pyrolysis of MGW was conducted using an auger reactor situated at the Fuel and Energy Research Laboratory, Central Queensland University's North Rockhampton campus. Detailed views of the reactor setup are depicted in Figures 2 and 3.

Figure 2. The pictorial view of the whole reactor setup used in the present study.

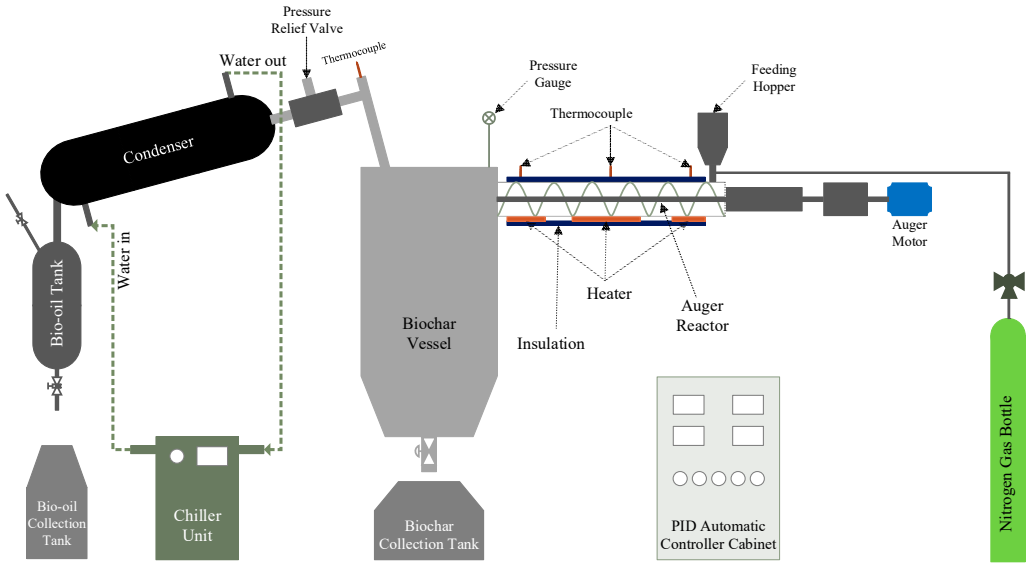

Figure 3. Schematic diagram of auger pyrolysis reactor system used in the present study.

The auger reactor is composed of four main sections: feeding, reactor, biochar collection, and condensing. The reactor core features a quartz tube, externally heated by an electrical ring furnace, which is insulated with an external sheet. The reactor measures 1300 mm in length and has an outer diameter of 100 mm. Temperature measurements throughout the reactor are taken using K-type thermocouples. Heating rates and temperatures are precisely controlled by a PID Automatic Controller. Nitrogen gas is supplied from a cylinder to purge oxygen from the system, regulated by a pressure control valve and an additional pressure regulator, maintaining a pressure of 30 kPa. This setting ensures that the operation remains at or near atmospheric pressure. A pressure gauge located above the 20 L biochar vessel monitors the internal pressure, and a pressure relief valve is in place to prevent over-pressurization and to protect the reactor from damage. For condensation, a chiller unit is used to convert vapor into bio-oil. The chiller operates within a temperature range of −5 to 20 °C.

2.3. Experimental Procedure

Each pyrolysis experiment utilized 2 kg of MGW, preceded by 15 min of nitrogen purging to eliminate any residual oxygen, rendering the system inert. The pyrolysis reaction occurred at 500 °C, facilitated by activated heating elements. The auger motor regulated residence time by controlling the screw's rotation speed. Resulting from pyrolysis, biochar and vapor were produced, with biochar collected post-process and vapor condensed to yield bio-oil. The following Equation (1) determined the bio-oil yield, Equation (2) calculated the biochar yield, and Equation (3) deduced the syngas yield, all based on mass measurements.

$$Yield\ of\ bio\text{-}oil\ (\%) = \frac{Mass\ of\ bio\text{-}oil}{Mass\ of\ feedstock} \times 100 \quad (1)$$

$$Yield\ of\ biochar\ (\%) = \frac{Mass\ of\ biochar}{Mass\ of\ feedstock} \times 100 \quad (2)$$

$$Yield\ of\ syngas\ (\%) = 100 - (Yield\ of\ bio\text{-}oil + Yield\ of\ biochar) \quad (3)$$

2.4. Characterization of MGW and Produced Bio-Oil

Both proximate and ultimate analyses were used to characterize the MGW after it had been sun-dried and shredded. Applying a modified version of the Van Soest method that was proposed by Abitbol et al. [25] was performed during the biochemical analysis of MGW so that the percentages of cellulose, hemicellulose, lignin, and extractives could be determined. For the characterization of produced bio-oil from fast pyrolysis of MGW, two analysis techniques, FTIR and GC-MS, were utilized. Various physicochemical properties of produced bio-oil were determined using different testing tools. The detailed description and working principle of the equipment used to characterize the MGW and produced bio-oil can be found in our previous work [26]. A list of this equipment, along with the respective analysis and the ASTM standards followed, are presented in Table 1.

Table 1. The characterization equipment and respective ASTM standards.

Analysis/Properties	ASTM Standards	Equipment
MGW		
Proximate analysis	D3172-07a	Thermogravimetric analyzer (Mettler Toledo TGA/SDTA 851)
Ultimate analysis	D5373	Vario Micro Cube CHNS analyzer
Higher heating value	D4809	Oxygen-bomb calorimeter
Bio-oil		
FTIR analysis	–	Perkin Elmer System One FTIR/ATR spectrum analyzer
GC-MS analysis	–	Varian CP3800 mass spectroscopy detector
Kinematic viscosity	D7042	Stabinger Viscometer SVM 3000
Density	D4052	Density meter DM40 Mettler Toledo
pH	E70	Omega DP24-pH meter
Cetane number	D613	Ignition quality tester
Water content	D2709	Centrifuge sigma
Flash point	D93B	Pensky Martins closed cup apparatus
Calorific value	D4809	Oxygen-bomb calorimeter

3. Results and Discussion

3.1. Characterization of MGW

The characterization of MGW was carried out by performing the proximate, ultimate, and biochemical analyses of MGW. These types of analyses are frequently used to establish whether a solid material is suitable for use as a fuel. Table 2 presents a summary of the findings from these analyses. A comparison was also made between the results obtained from the present study and the results obtained for similar sorts of solid waste, such as royal poinciana seed (RPS) [27], banana leaves (BL) [28], and pecan nutshell (PNS) [29]. According to the proximate analysis presented in Table 2, the MGW contains a high volatile content of 69.57%. Like other biomass waste utilized in fast pyrolysis experiments, the

volatile matter in MGW is equivalent to RPS (73.15%), BL (73.05%), and PNS (67.93%). The higher the percentage of volatile matter in a material, the greater the appropriateness of the material for the pyrolysis process. The volatile matter present in a material is decomposed during the pyrolysis process and forms various gaseous elements, which can be condensed to produce valuable liquid products [30]. The ash content in the MGW is 0.93%, which is lower than other biomass wastes. When there is a considerable amount of soil adhering to a material, the ash content tends to be higher [31]. For this reason, the MGW used in this study was washed thoroughly before usage to remove any soil attached to it. Additionally, the reduced amounts of moisture content and fixed carbon that are present in dried MGW contribute to the material's increased suitability for the pyrolysis process.

Table 2. Properties of dried MGW in comparison with literature data.

Analysis	Property	MGW	Royal Poinciana Seed [27]	Banana Leaves [28]	Pecan Nutshell [29]
Proximate (wt%)	Moisture	9.72	6.21	8.4	3.32
	Volatile matter	69.57	73.15	73.05	67.93
	Fixed carbon [a]	19.78	17.7	7.26	29.69
	Ash	0.93	3.02	11.29	2.47
Ultimate (wt%)	Carbon	47.32	52.12	43.28	49.22
	Hydrogen	5.14	5.86	6.83	5.59
	Nitrogen	0.42	5.1	1.28	0.65
	Oxygen [a]	47.06	36.42	48.31	41.92
	Sulphur	0.06	0.5	0.3	0.14
Biochemical (wt%)	Cellulose	37.53	27	43.34	14.99
	Hemicellulose [a]	22.34	44.21	34.34	27.59
	Lignin	24.92	12	15	48.37
	Extractives	15.21	16.32	7.32	9.05
	HHV (MJ/kg)	18.24	20.52	17.8	19.39

[a] By difference.

The ultimate analysis of MGW reveals that it contains a high carbon content of 47.32% and a hydrogen content of 5.14%. These results are comparable with the published literature data on similar types of material. Nitrogen is contained in MGW at a concentration of 0.42%, and sulphur is present at a concentration of 0.06%. Because nitrogen and sulphur act as sources of NO_X and SO_X pollution, these low values indicate that MGW is environmentally friendly and that it can be used in the pyrolysis process without negatively impacting the environment [32]. The biochemical analysis of MGW shows that the MGW contains 37.53%, 22.34%, 24.92%, and 15.21% of cellulose, hemicellulose, lignin, and extractives, respectively. The lignin content in MGW is higher compared to the reported lignin content values for RPS [27] and BL [28]. According to Shahbaz et al. [33], the material that contains high lignin has the potential to produce a higher amount of bio-oil when subjected to pyrolysis. The higher heating value (HHV) of MGW was found to be 18.24 MJ/kg. When compared to the value that Singh et al. [28] reported for BL, this value is just a little higher. On the other hand, the HHV of MGW is lower in comparison to that of other types of solid wastes, such as RPS and PNS, which have 20.52 MJ/kg and 19.39 MJ/kg of HHV, respectively. The amount of carbon and hydrogen that are present in a material are two factors that often have an effect on the HHV of the material. A higher carbon content results in a greater amount of heat generated during the combustion process, which leads to a higher HHV [34].

3.2. Yield of Pyrolysis Products

3.2.1. Effect of Residence Time

The effect of residence time on the yields of bio-oil, biochar, and syngas derived from MGW is shown in Figure 4. The pyrolysis temperature was kept at 500 °C, and a particle

size of 2 mm was used for each residence time experiment. Experiments were carried out in triplicate for each of the conditions, and the error bar in Figure 4 illustrates the standard deviation at each of the conditions. As can be observed in Figure 4, the bio-oil yield increases with increasing residence time and achieves its maximum yield (39.86%) at 3 min. Further increasing the residence time decreases the bio-oil yield. This is due to secondary reactions like cracking and re-polymerization that have taken place during the pyrolysis process when longer residence times are applied. This results in an increase in the yield of syngas, while simultaneously resulting in a decrease in the amount of bio-oil produced [35]. The yield of syngas increased gradually from 27.5% to 38.35% when the residence time was varied from 1 min to 4 min. When looking at the yield of biochar, the opposite tendency could be observed. As the residence time increases, there is a substantial drop in the amount of biochar produced. The yields of fast pyrolysis products have been shown to be significantly affected by residence time in prior studies using similar feedstocks [13,36,37].

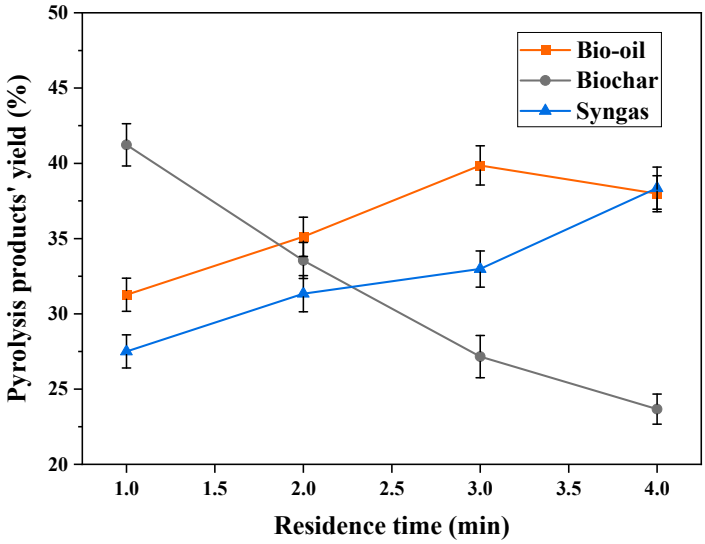

Figure 4. Effect of residence time on the yields of pyrolysis products.

The outcomes of the present study are in line with the published literature data. It is usually considered that short residence times are favorable for the production of bio-oil from pyrolysis. During a fast pyrolysis process, vapors are prone to subsequent cracking. To prevent further cracking, it is ideal to use short residence times [38]. However, it is unlikely that complete decomposition of feedstock can be achieved during very short residence times due to limitations in heat transport at the particle surface. For this reason, the residence time should be longer than the vapor residence time in the reactor [39].

3.2.2. Effect of Particle Size

Figure 5 depicts the quantities of bio-oil, biochar, and syngas produced in relation to the size of the feedstock particles. The temperature and residence time were maintained at 500 °C and 3 min, respectively, for each experiment involving different particle sizes. Three experiments were conducted for each condition, and the error bars in Figure 5 indicate the standard deviation. Figure 5 demonstrates that the bio-oil yield exhibits a modest rise from 37.45% to 39.86% as the particle size grows up to 2 mm. However, it quickly declines to 33.66% as the particle size of MGW continues to increase. Using larger particles causes uneven heating, which leads to an incomplete breakdown and a reduced bio-oil output [40].

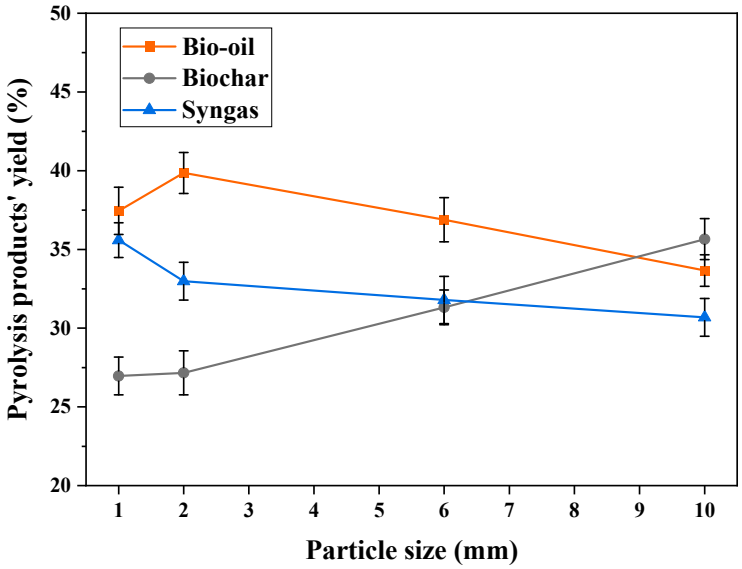

Figure 5. Effect of particle size on the yields of pyrolysis products.

A contrasting pattern emerged concerning biochar yield, which increased from 26.96% to 35.65% as the MGW particle size enlarged from 1 mm to 10 mm. Larger particles induce more heat resistance, resulting in lower internal temperatures and thus higher biochar yields [17]. Figure 5 illustrates a gradual decline in syngas yield with increasing particle size. The study found the highest syngas yield (35.59%) with the smallest particle size (1 mm), attributed to small particles being prone to overheating and swift dispersion [41]. Similar observations regarding the particle size's impact on pyrolysis product yields have been made by various researchers using analogous feedstocks to MGW [42–44]. These findings align closely with those of the current study.

3.3. Characterization of Bio-Oil

3.3.1. FTIR Analysis

The effect of residence time and particle size on the functional groups of various chemical compounds present in the obtained bio-oils is illustrated by FTIR spectra. For this comparative analysis to have any meaning, it must be pointed out that the spectra were not analyzed in a quantitative manner. That is why this FTIR analysis is a good source of knowledge about how various compounds are affected by residence time and particle size variation. The spectra for bio-oil obtained at different residence times and particle sizes are shown in Figs. 6 and 7, respectively. It is seen from both figures that the shape and position of various absorption bands in the spectra are consistent. However, there are differences in intensity between individual modes, which appears to reveal a significant impact of residence time and particle size on the relative contribution from various chemical groups.

Figures 6 and 7 demonstrate that the main functional groups are situated within distinct wavenumber ranges, notably ranging from 700 cm^{-1} to 1800 cm^{-1} and from 2800 cm^{-1} to 3600 cm^{-1}. The wide absorbance signals detected in the range of 3300 cm^{-1} to 3600 cm^{-1} correspond to stretching vibrations of O–H bonds, while peaks in the range of 1200 cm^{-1} to 1450 cm^{-1} indicate stretching vibrations of C–O bonds. The appearance of alcohols and phenols in the bio-oils can be ascribed to the stretching vibrations of both O–H and C–O bonds [45]. The presence of alkanes in the bio-oils is indicated by C–H stretching vibrations in the range of 2800 cm^{-1} to 3000 cm^{-1} and C–H bending vibrations in the range of 1450 cm^{-1} to 1550 cm^{-1} [46]. C–O stretching vibrations about 1600 cm^{-1} can be used to detect the presence of ketones, aldehydes, and esters [47]. In addition, carboxylic acids are characterized by prominent peaks at about 1000 cm^{-1}, which correspond to the stretching vibrations of O–H and C–O bonds in the fingerprint area [48].

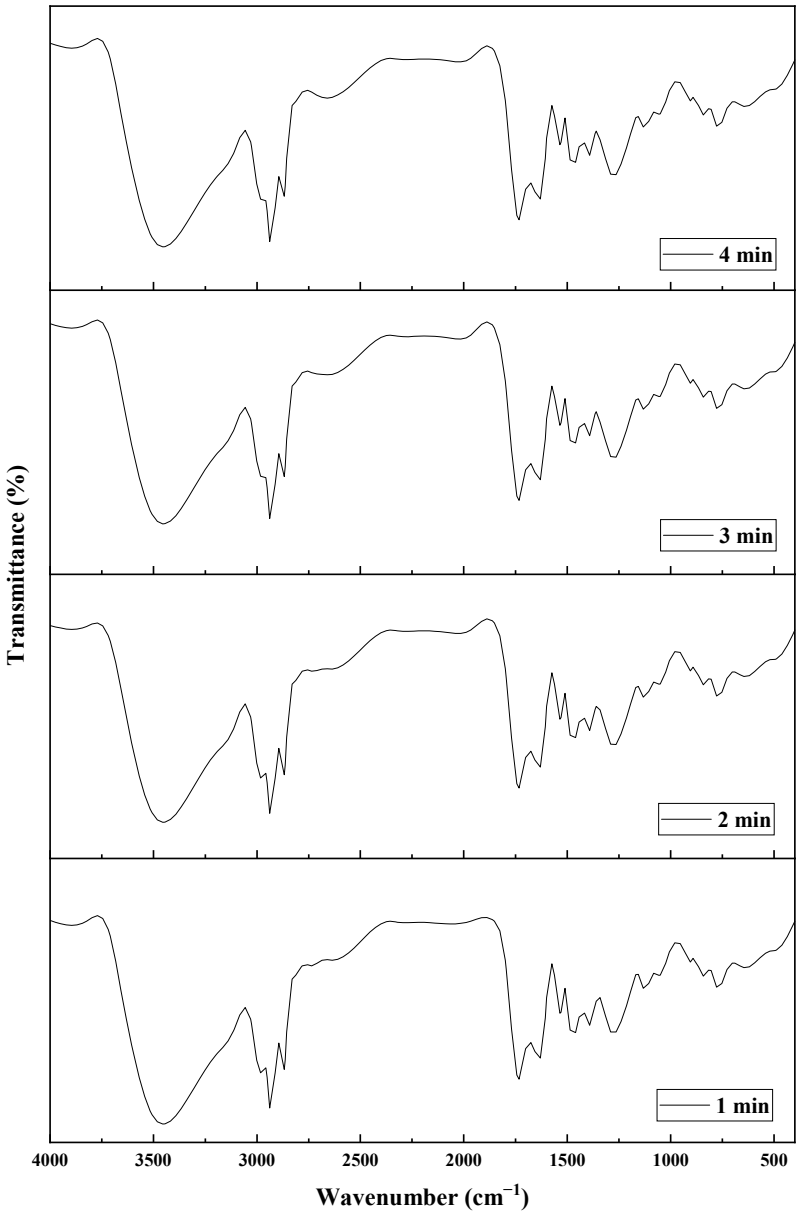

Figure 6. The FTIR spectra for bio-oils obtained at different residence times.

The presence of aromatic compounds can be identified by the existence of the C–C stretching vibration at 1750 cm^{-1} and the characteristic sharp peak at 1650 cm^{-1}. The observation of aromatic C–H stretching vibration in the region of wavelengths between 600 cm^{-1} and 900 cm^{-1} gives rise to the hypothesis that aromatic polycyclic hydrocarbons are present in the bio-oil samples [49]. Finally, it can be said that MGW-derived bio-oil had a similar FTIR spectrum to that of bio-oil derived from other similar types of feedstocks, such as banana peel [50], potato peel [51], and lebbek tree waste [52].

The FTIR spectra are greatly affected by the residence time of the fast pyrolysis process and the particle size of MGW. The O–H stretching vibrations increase sharply with increasing residence time up to 3 min and decrease slightly with further increases in the residence time. When comparing the FTIR spectra obtained at different particle sizes, the particle size of 2 mm exhibits the lowest absorption band. There is no significant effect of residence time observed on C–O stretching vibrations. For particle sizes of 1, 6, and 10 mm, the C–O stretching vibrations have almost the same values, whereas a particle size of 2 mm has a higher value compared to other particle sizes. The values of O–H and C–O stretching vibrations reveal that more stable bio-oil was obtained when a particle size of

2 mm was used [53]. Similar trends were followed by the C–C stretching vibration and the C–H stretching vibration as C–O stretching vibrations. Thus, it can be said that the bio-oil obtained using a particle size of 2 mm has more potential for use as engine fuel [54].

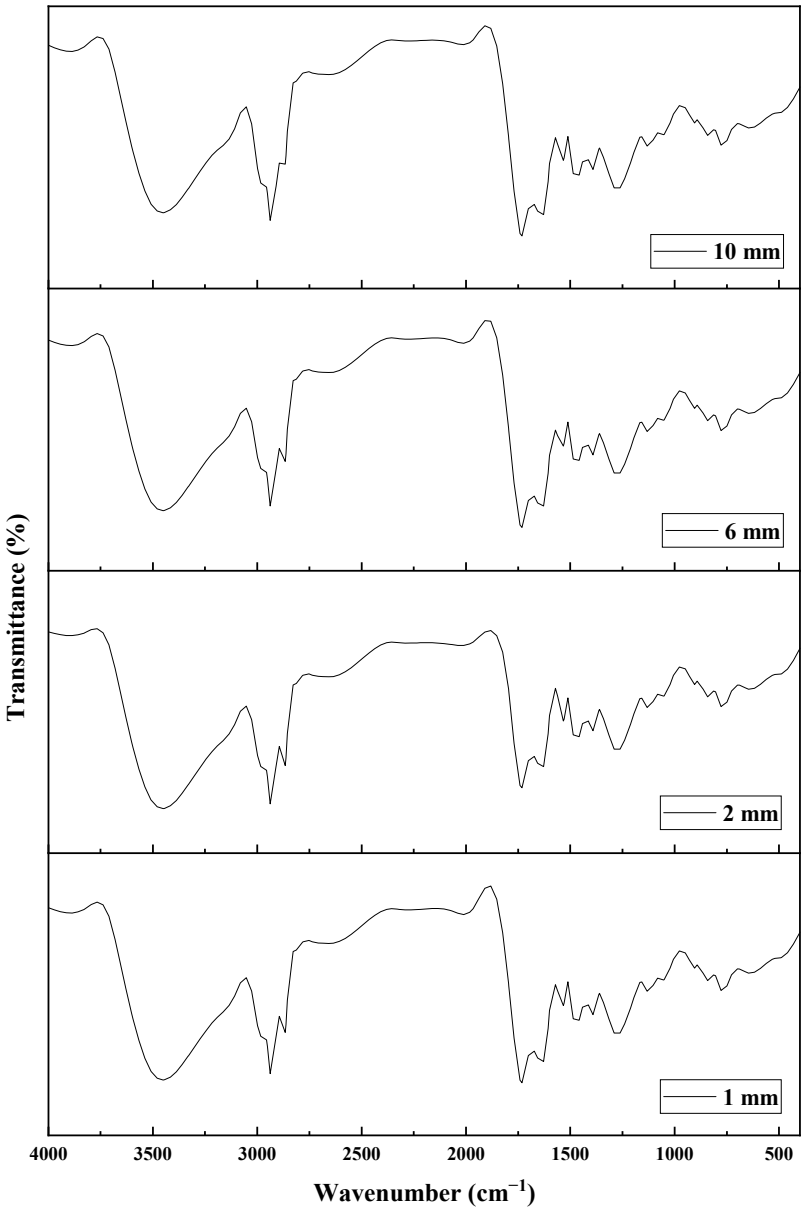

Figure 7. The FTIR spectra for bio-oils obtained at different particles sizes of MGW.

3.3.2. GC–MS Analysis

FTIR analysis enables rapid classification of various chemical compounds present in bio-oil, while quantitative analysis can be conducted using GC-MS [55]. Therefore, the bio-oils obtained at different residence times and particle sizes underwent GC-MS analysis to identify their chemical composition. Compounds with significant peak areas and at least 80% similarity were compiled for analysis. While the peak areas provide approximate concentrations, they offer valuable insights into the relative abundances of the compounds. To enhance accuracy, peak areas from triplicate tests were averaged, ensuring consistent data representation.

Listed in Table 3 are the major chemical compounds found in fast-pyrolysis-processed MGW-derived bio-oils at various residence times and particle sizes.

Table 3. List of chemical compounds found in bio-oils obtained from the fast pyrolysis of MGW at different residence times and particle sizes.

Chemical Compound	Molecular Formula	Retention Time (min)	Peak Area (%)—Residence Times				Peak Area (%)—Particle Sizes			
			1 min	2 min	3 min	4 min	1 mm	2 mm	6 mm	10 mm
Alcohols										
propan-1-ol	C_3H_8O	7.15	0.91	0.93	0.99	0.89	0.97	0.99	1.01	1.05
1-tetradecanol	$C_{14}H_{30}O$	34.29	1.07	1.05	1.23	1.11	1.29	1.23	1.19	1.21
1-heptadecanol	$C_{17}H_{36}O$	40.99	1.63	1.75	1.61	1.69	1.54	1.61	1.71	1.84
Aldehydes										
3-hydroxypropanal	$C_3H_6O_2$	14.75	0.59	0.61	0.63	0.59	0.64	0.63	0.61	0.59
succinaldehyde	$C_4H_6O_2$	18.13	0.74	0.72	0.71	0.81	0.69	0.71	0.7	0.69
Alkanes										
cyclopropane	C_3H_6	5.44	0.54	0.56	0.51	0.57	0.49	0.51	0.49	0.56
undecane	$C_{11}H_{24}$	16.61	0.74	0.69	0.75	0.67	0.71	0.75	0.77	0.87
dodecane	$C_{12}H_{26}$	23.92	0.81	0.84	0.79	0.91	0.77	0.79	0.83	0.82
tetradecane	$C_{14}H_{30}$	29.03	0.59	0.57	0.67	0.54	0.61	0.67	0.52	0.54
pentadecane	$C_{15}H_{32}$	34.59	0.39	0.36	0.42	0.31	0.47	0.42	0.37	0.41
hexadecane	$C_{16}H_{34}$	39.65	0.21	0.11	0.31	0.23	0.29	0.31	0.29	0.27
Aromatics										
benzene	C_6H_6	6.57	1.75	1.77	1.89	1.76	1.71	1.89	1.77	1.78
pyridine	C_5H_5N	9.12	0.73	0.69	0.76	0.67	0.72	0.76	0.73	0.69
pyrrole	C_4H_5N	11.35	0.43	0.51	0.39	0.51	0.33	0.39	0.37	0.41
toluene	C_7H_8	14.21	1.07	1.01	1.11	0.99	1.01	1.11	1.15	0.91
ethylbenzene	C_8H_{10}	18.34	0.32	0.33	0.41	0.24	0.42	0.41	0.39	0.32
benzofuran	C_8H_6O	23.41	0.21	0.19	0.23	0.11	0.11	0.23	0.29	0.24
Carboxylic Acids										
1-allyl cyclopropane carboxylic acid	$C_7H_{10}O_2$	18.72	0.51	0.52	0.49	0.53	0.51	0.49	0.52	0.5
14-pentadecynoic acid, methyl ester	$C_{17}H_{34}O_2$	42.67	0.84	0.81	0.77	0.79	0.78	0.77	0.81	0.84
hexadecenoic acid, methyl ester	$C_{17}H_{34}O_2$	44.98	0.54	0.51	0.53	0.52	0.61	0.53	0.56	0.49
octadecanoic acid, methyl ester	$C_{19}H_{38}O_2$	48.41	0.45	0.47	0.41	0.46	0.42	0.41	0.37	0.53
Esters										
ethyl acetate	$C_4H_8O_2$	9.49	0.54	0.51	0.59	0.55	0.47	0.59	0.57	0.61
2-oxopropyl acetate	$C_5H_8O_3$	16.77	0.59	0.49	0.61	0.58	0.57	0.61	0.53	0.49

Table 3. *Cont.*

Chemical Compound	Molecular Formula	Retention Time (min)	Peak Area (%)—Residence Times				Peak Area (%)—Particle Sizes			
			1 min	2 min	3 min	4 min	1 mm	2 mm	6 mm	10 mm
Ketones										
3-Hexanone	$C_6H_{12}O$	8.43	0.65	0.63	0.66	0.61	0.61	0.66	0.65	0.67
ethanone,1-(2-furanyl)	$C_6H_6O_2$	8.81	1.01	1.12	1.23	1.14	1.19	1.23	1.21	1.17
cyclopentanone,2-methyl	$C_6H_{10}O$	11.53	1.27	1.29	1.3	1.25	1.23	1.3	1.29	1.27
2-cyclopenten-1-one,3-methyl	C_6H_8O	12.99	0.99	1.01	1.11	1.05	1.01	1.11	1.09	1.12
2-cyclopenten-1-one,2-methyl	C_6H_8O	14.19	0.74	0.77	0.79	0.67	0.71	0.79	0.78	0.76
Phenols										
phenol	C_6H_6O	17.12	1.45	1.41	1.47	1.39	1.42	1.47	1.39	1.47
phenol, 2-methyl	C_7H_8O	20.77	1.2	1.23	1.21	1.27	1.17	1.21	1.14	1.19
phenol, 2,3-dimethyl	$C_8H_{10}O$	22.79	1.67	1.69	1.76	1.75	1.56	1.76	1.78	1.79
2-methoxy-5-methyl phenol	$C_8H_{10}O_2$	23.56	1.73	1.74	1.71	1.72	1.65	1.71	1.45	1.67
phenol, 4-ethyl-2-methoxy	$C_9H_{12}O_2$	28.91	0.97	0.94	0.99	1.01	1.01	0.99	0.89	0.92
phenol,2-methoxy-4-propyl	$C_{10}H_{14}O_2$	36.45	1.35	1.29	1.32	1.29	1.11	1.32	1.43	1.31
3-phenyl-5-t-butylpyridazine	$C_{14}H_{16}N_2$	38.69	1.35	1.37	1.42	1.32	1.34	1.42	1.41	1.39
Polycyclic Aromatic Hydrocarbons (PAH)										
naphthalene	$C_{10}H_8$	27.13	0.97	0.99	1.05	0.91	1.01	1.05	1.02	0.99
2-methylnaphthalene	$C_{11}H_{10}$	29.42	0.69	0.67	0.71	0.84	0.69	0.71	0.77	0.73
biphenyl	$C_{12}H_{10}$	31.63	0.45	0.49	0.47	0.48	0.49	0.47	0.51	0.45
1-methylnaphthalene	$C_{11}H_{10}$	33.51	0.48	0.53	0.45	0.51	0.51	0.45	0.43	0.56
acenaphthene	$C_{12}H_{10}$	37.81	0.42	0.41	0.51	0.49	0.49	0.51	0.49	0.51
fluorene	$C_{13}H_{10}$	39.97	0.97	1.02	0.97	0.93	0.99	0.97	0.91	0.87
anthracene	$C_{14}H_{10}$	41.67	0.84	0.81	0.79	0.81	0.84	0.79	0.81	0.79
pyrene	$C_{16}H_{10}$	43.78	0.35	0.41	0.43	0.39	0.31	0.43	0.33	0.41

The analysis reveals significant compounds across various classes, including hydrocarbons, oxygenates, acids, and others. Notable hydrocarbons, such as benzene (retention time: 3.42 min, peak area: 5.67%), toluene (retention time: 5.88 min, peak area: 2.45%), and xylene (retention time: 8.35 min, peak area: 1.73%), enhance the energy density of the bio-oil, making it suitable for fuel production [56]. Oxygenated compounds, including phenol (retention time: 12.25 min, peak area: 12.37%), cresol (retention time: 14.60 min, peak area: 9.56%), and guaiacol (retention time: 16.75 min, peak area: 7.88%), contribute to the bio-oil's chemical complexity and potential for industrial applications despite lowering its overall energy content [57].

The presence of acids like acetic acid (retention time: 19.50 min, peak area: 15.44%), formic acid (retention time: 20.85 min, peak area: 4.23%), and propionic acid (retention time: 22.10 min, peak area: 3.68%) presents challenges for fuel use due to increased acidity and corrosion issues [58]. However, other compounds, like furfural (retention time: 24.65 min, peak area: 2.12%) and 2,3-butanedione (retention time: 26.80 min, peak area: 1.37%), offer valuable opportunities for chemical production. Furfural, for instance, is crucial in producing furan-based chemicals and biofuels [59]. This diverse chemical composition underscores the need for upgrading processes like hydrodeoxygenation (HDO) to reduce oxygen content and acidity, thus improving bio-oil's suitability as a transportation fuel. Understanding these compositional trends helps optimize pyrolysis parameters to enhance the yield of desirable compounds, thereby maximizing the bio-oil's economic and practical applications.

These intricate details highlighted by GC-MS analysis shed light on the bio-oil's rich chemical composition. However, due to the low concentrations of these valuable components, they are not economically extractable in their pure form. Their primary value lies in their heating potential. Employing certain techniques, such as staged condensation with stepwise decreasing cooling temperatures, may lead to enriched fractions, such as phenolics, which can be used to produce resol resins [60]. This approach can enhance the overall value of the bio-oil through targeted product transformation.

Following the GC-MS analysis, the chemical compounds detected were classified into nine distinct functional groups, offering valuable insights into the composition of the bio-oil. Figures 8 and 9 visually represent the distribution of chemical compounds across various functional groups, providing a comprehensive view of their relative abundance under different residence times and particle sizes. The results underscore the diverse nature of the chemical compounds present, encompassing phenolic, aromatic, oxygenated, and hydrocarbon compounds, among others. Particularly noteworthy is the prevalence of phenolic compounds, which emerge as the dominant functional group in both analyses, closely followed by aromatic compounds. This substantial presence of phenol within the bio-oil suggests promising potential for its refinement into higher-quality fuel products, indicative of its commercial viability [61]. However, it is important to note that regulatory trends have increasingly restricted the allowed concentration of phenolic and aromatic compounds in transportation fuels. While phenols and mono-aromatics have historically been valued for their properties in fuels, their desirability has diminished due to these regulatory changes. Thus, the focus should also include the potential for converting these compounds into other valuable chemical products beyond transportation fuels. Interestingly, the data also reveal nuanced trends. While there is a minor increase in phenol content with longer residence times up to 3 min, this trend reverses beyond this threshold. Additionally, the analysis highlights the influence of particle size variation, with the highest phenol levels observed with a particle size of 2 mm. This abundance of phenolic compounds can be attributed to the breakdown of lignin structures within the feedstock during the pyrolysis process. Furthermore, the optimal residence time of 3 min emerges as a crucial factor in facilitating efficient decomposition of MGW, resulting in the highest yield of phenolic compounds. These findings not only deepen our understanding of the chemical composition of bio-oil but also provide valuable insights for optimizing pyrolysis processes to enhance the yield of desirable chemical compounds for various applications.

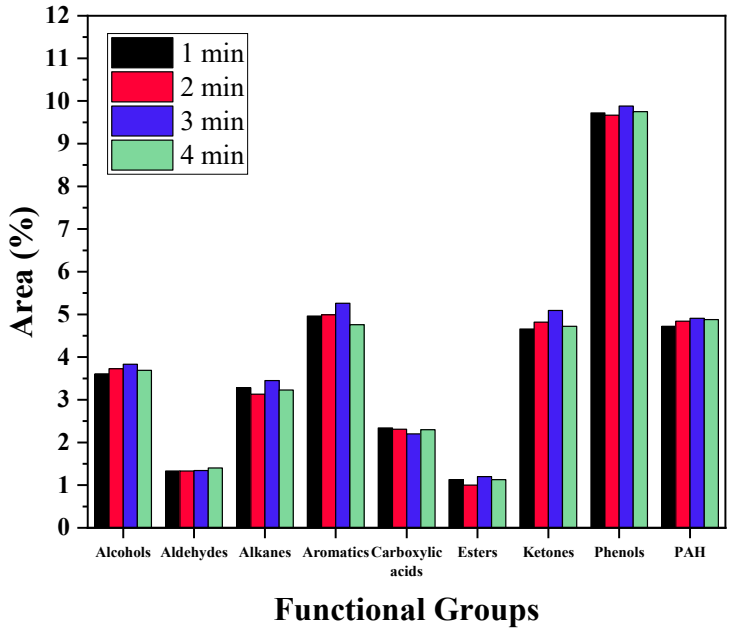

Figure 8. Major functional groups present in the bio-oils obtained at different residence times.

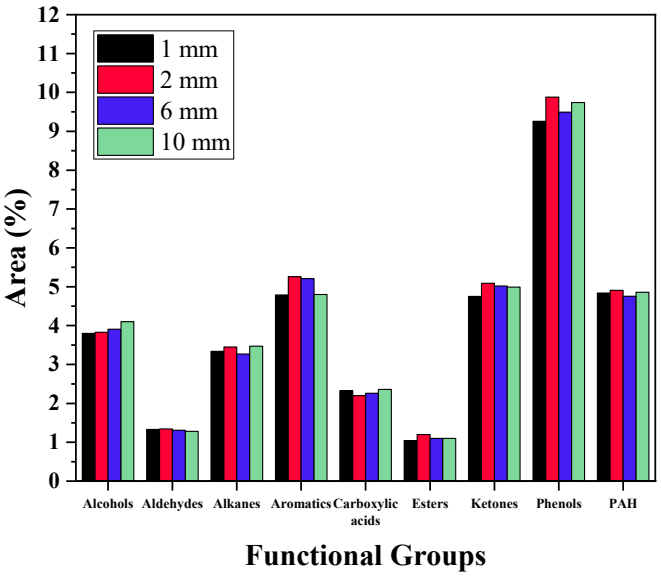

Figure 9. Major functional groups present in the bio-oils obtained using different particle sizes of MGW.

An important component of the produced bio-oils is aromatic compounds, both monocyclic and polycyclic. The aromatic functional group is important because these compounds may have far-reaching positive effects on the economy or the environment [62]. The obtained bio-oils contained oxygenated compounds at detectable concentrations. High levels of oxygenated compounds in a fuel can cause several issues, including decreased energy density, calorific value, and storage stability, as well as increased acidity [63]. In the condensation phase, bio-oil's acidic chemicals result in rapid polymerization reactions. This behavior can be explained by the fact that bio-oil contains both volatile functional groups and free oligomer radicals. Because of these concerns, the use of bio-oil as an engine fuel is severely limited as it ages [64]. The presence of acidic compounds in bio-oil makes it hard to store bio-oil for extended periods [65]. Therefore, these unwanted compounds need to be extracted from the bio-oils that have been obtained so that they can be improved. The

increase in residence time decreased the contents of carboxylic acids in the obtained bio-oils. This is qualitatively in line with the results obtained by Salehi et al. [66] and Wang et al. [67].

The obtained bio-oils also contain moderate amounts of hydrocarbons. The bio-oil that was produced with a combination of a residence time of 3 min and a particle size of 2 mm had the highest concentration of hydrocarbons. The relative quality of hydrocarbon materials is brought down by the fragile C–H bonds, which have a greater propensity to be broken during shorter residence times and with larger particle sizes [68].

3.3.3. Physicochemical Properties Analysis

The analysis of physicochemical properties of bio-oils aimed to explore how residence times and particle sizes impact the bio-oils' quality. These properties were compared against standard fuel benchmarks to evaluate the bio-oils' suitability for use as engine fuels. Table 4 outlines the physicochemical properties of bio-oils produced from fast pyrolysis of MGW under various residence times and particle sizes, alongside standard fuel properties.

Kinematic viscosity and density emerge as pivotal indicators for assessing fuel suitability for engine applications. Kinematic viscosity plays a crucial role in determining atomization and spray characteristics, as well as overall engine efficiency. Oils with high viscosity can impede fuel injector efficiency due to reduced atomization during fuel delivery. Conversely, engine efficiency and combustion characteristics are influenced by fuel density. An analysis of Table 4 reveals a decreasing trend in both kinematic viscosity and density with increasing residence time up to 3 min, followed by a slight increase thereafter. The residence time of 3 min is also the optimum for maximum bio-oil yield. The reason for obtaining the best kinematic viscosity and density at this residence time is that the MGW had sufficient time to be disintegrated properly to form liquid hydrocarbons, but not so much as to lead to further cracking into C1–4 components [69]. In terms of particle size variation, 2 mm provided the best kinematic viscosity and density as 12.17 cSt and 1.13 g/cc, respectively. Further increasing the particle from 2 mm increased both kinematic viscosity and density. This can be attributed to larger particles being heat-resistant, which ultimately degrades the quality of the bio-oil [70]. The comparison between obtained bio-oils and standard fuel reveals that changes to the experimental conditions have resulted in improvements in the values of kinematic viscosity and density; however, these values still need to be significantly improved before they can be considered comparable to those of conventional fuel for engines.

Despite changes in residence time and particle size, the pH values of the bio-oils remained relatively unchanged. This stability correlates with the levels of carboxylic acid compounds identified through GC-MS analysis. Maintaining a neutral pH is crucial for ensuring the safe storage and transportation of fuels. However, the consistently low pH values observed in the bio-oils obtained in this study indicate their acidic nature. This acidity could potentially impact their handling and usability in various applications. Interestingly, these findings are in line with previous research conducted by DeSisto et al. [71], Abdullahi et al. [72], and Salehi et al. [66], where similar feedstocks were used and comparable acidic characteristics were observed in the resulting bio-oils. This consistency across studies reinforces the understanding of the chemical composition and properties of bio-oils derived from similar biomass sources.

The cetane number is another essential parameter that is used to characterize a fuel. The total amount of NO_X emissions that are produced when a fuel is combusted in an engine is directly proportional to the cetane number of the fuel. The influence of residence time and particle size on the values of cetane number of the produced bio-oils was not found to be significant in its impact, and all of the values fall within the range of engine fuel. Rodriguez et al. came to a conclusion that was parallel to the findings of the present study [73].

Regarding the water content found in the produced bio-oils, it was observed that all bio-oils exhibit relatively higher percentages of water. For instance, bio-oils obtained using a particle size of 10 mm contained around 25.93% water, whereas those obtained with a

residence time of 4 min had approximately 29.51% water content. Typically, the water content in bio-oils falls within the range of 15% to 30% [74]. Therefore, the water content observed in the bio-oils from this study falls within this established range. The presence of water in the bio-oil primarily results from the volatilization of moisture present in the feedstock and dehydration reactions occurring during the fast pyrolysis process. There is an increasing trend in water content that was observed with increasing residence time, and the opposite trend was observed for increasing particle size. This can be attributed to dehydration reactions getting ample time to take place when the residence time is higher, which ultimately generates a greater amount of water [75].

The water content of a fuel plays a significant role in determining its flash point and calorific value. The analysis revealed that bio-oils obtained under longer residence times and smaller particle sizes exhibited higher flash points, indicating their suitability for safe storage at ambient temperatures [76]. The calorific values of the bio-oils ranged between 24.99 MJ/kg and 25.89 MJ/kg, aligning with previously published data on similar feedstocks [77–79]. Although there was a minor impact of residence time and particle size on the calorific value, this observation is likely attributable to variations in water content. Higher water content necessitates more energy for evaporation, consequently reducing the calorific value of the bio-oil [80].

Table 4. The physicochemical properties of MGW-derived bio-oils obtained at different residence times and particle sizes and of standard fuels.

Properties	Residence Times				Particle Sizes				ASTM Grade G [81]	ASTM Grade D [82]	Heavy Fuel Oil [83]	Light Fuel Oil [75]
	1 min	2 min	3 min	4 min	1 mm	2 mm	6 mm	10 mm				
Kinematic viscosity @40 °C (cSt)	13.21	12.78	12.17	12.51	12.68	12.17	12.99	13.54	Maximum 125	Maximum 125	180–420	2–4.5
Density @30 °C (g/cc)	1.17	1.14	1.13	1.14	1.17	1.13	1.19	1.21	1.1–1.3	1.1–1.3	0.99–0.995	Maximum 0.845
pH	3.7	3.5	3.6	3.7	3.5	3.6	3.6	3.7	–	–	–	–
Cetane number	38	38	40	39	39	40	38	39	–	–	35–55	38–40
Water content (wt%)	26.43	27.87	28.72	29.51	28.97	28.72	26.34	25.93	Maximum 30	Maximum 30	~0	~0
Flash point (°C)	86	87	90	91	91	90	85	83	–	–	90–180	52–82
Calorific value (MJ/kg)	25.81	25.45	25.13	24.99	24.51	25.13	25.71	25.89	Minimum 15	Minimum 15	40.6	42.6

Upon analyzing the physicochemical properties of the bio-oils derived from MGW at different residence times and particle sizes, it becomes evident that these bio-oils are not yet suitable for direct use in engines. However, their potential as efficient heating sources in boilers and furnaces remains promising. To transition these bio-oils into engine-compatible fuels, upgrading processes are indispensable. Various techniques, such as HDO [84], catalytic cracking [85], distillation [86], esterification [87], and emulsification [88], offer ways of enhancing the quality of the obtained bio-oils. Implementing one of these methods to upgrade the bio-oils from this study is envisioned as a future research direction for the authors. Such efforts aim to unlock the full potential of these bio-oils, rendering them suitable for diverse applications while minimizing environmental impact.

4. Conclusions

This study conducted on the fast pyrolysis of MGW in an auger reactor has yielded several significant findings. These results highlight the potential of MGW as a feedstock for bio-oil production and the various factors influencing the yield and quality of the produced bio-oil. The following key conclusions can be drawn from this research:

- MGW contained high carbon (47.32%) and lignin (24.92%) content, highlighting its suitability for pyrolysis.
- A maximum bio-oil yield of 39.86% was achieved with a residence time of 3 min and a particle size of 2 mm, optimizing the pyrolysis reaction and heat transfer.
- Phenolic compounds increased with longer residence times and larger particle sizes, while acidic compounds decreased.
- The presence of hydrocarbons like benzene (5.67% peak area) and toluene (2.45% peak area) indicates potential for fuel production.
- High acetic acid content (15.44% peak area) suggests challenges related to acidity that must be addressed for fuel applications.

- Bio-oils exhibited high viscosity and water content, necessitating upgrading for engine use but suitable for heating applications in boilers and furnaces.
- Upgrading methods, such as hydrodeoxygenation, catalytic cracking, distillation, esterification, and emulsification, are suggested to enhance bio-oil quality for broader applications.

Author Contributions: Conceptualization, M.M.H.; Methodology, M.I.J.; Validation, M.M.K.K.; Formal analysis, M.M.H.; Investigation, M.M.H.; Resources, M.I.J.; Writing—original draft, M.M.H.; Writing—review & editing, M.G.R., M.I.J. and M.M.K.K.; Supervision, M.G.R. All authors have read and agreed to the published version of the manuscript.

Funding: This research received no external funding.

Data Availability Statement: The original contributions presented in the study are included in the article, further inquiries can be directed to the corresponding author.

Acknowledgments: The authors express their gratitude to CQUniversity, Australia, for extending financial support to Mohammad Mehedi Hasan through a Research Training Program (RTP) Scholarship. Additionally, the authors appreciate the provision of experimental facilities by CQUniversity's Fuel and Energy Research Group.

Conflicts of Interest: The authors declare no conflict of interest.

References

1. Velghe, I.; Carleer, R.; Yperman, J.; Schreurs, S. Study of the pyrolysis of municipal solid waste for the production of valuable products. *J. Anal. Appl. Pyrolysis* **2011**, *92*, 366–375. [CrossRef]
2. Jahirul, M.I.; Brown, R.J.; Senadeera, W.; Ashwath, N.; Rasul, M.G.; Rahman, M.M.; Hossain, F.M.; Moghaddam, L.; Islam, M.A.; O'Hara, I.M. Physio-chemical assessment of beauty leaf (*Calophyllum inophyllum*) as second-generation biodiesel feedstock. *Energy Rep.* **2015**, *1*, 204–215. [CrossRef]
3. Jahirul, M.I.; Rasul, M.G.; Chowdhury, A.A.; Ashwath, N. Biofuels Production through Biomass Pyrolysis—A Technological Review. *Energies* **2012**, *5*, 4952–5001. [CrossRef]
4. Cepic, Z.; Nakomcic-Smaragdakis, B.; Miljkovic, B.; Radovanovic, L.; Djuric, S. Combustion characteristics of wheat straw in a fixed bed. *Energy Sources Part A Recovery Util. Environ. Eff.* **2016**, *38*, 1007–1013. [CrossRef]
5. Tanoh, T.S.; Ait Oumeziane, A.; Lemonon, J.; Escudero Sanz, F.J.; Salvador, S. Green Waste/Wood Pellet Pyrolysis in a Pilot-Scale Rotary Kiln: Effect of Temperature on Product Distribution and Characteristics. *Energy Fuels* **2020**, *34*, 3336–3345. [CrossRef]
6. Aysu, T.; Durak, H. Catalytic pyrolysis of liquorice (*Glycyrrhiza glabra* L.) in a fixed-bed reactor: Effects of pyrolysis parameters on product yields and character. *J. Anal. Appl. Pyrolysis* **2015**, *111*, 156–172. [CrossRef]
7. Hasan, M.M.; Rasul, M.G.; Khan, M.M.K.; Ashwath, N.; Jahirul, M.I. Energy recovery from municipal solid waste using pyrolysis technology: A review on current status and developments. *Renew. Sustain. Energy Rev.* **2021**, *145*, 111073. [CrossRef]
8. Khan, S.; Kay, L.A.N.; Qureshi, K.M.; Abnisa, F.; Wan Daud, W.M.A.; Patah, M.F.A. A review on deoxygenation of triglycerides for jet fuel range hydrocarbons. *J. Anal. Appl. Pyrolysis* **2019**, *140*, 1–24. [CrossRef]
9. Brassard, P.; Godbout, S.; Raghavan, V. Pyrolysis in auger reactors for biochar and bio-oil production: A review. *Biosyst. Eng.* **2017**, *161*, 80–92. [CrossRef]
10. Tripathi, M.; Sahu, J.N.; Ganesan, P. Effect of process parameters on production of biochar from biomass waste through pyrolysis: A review. *Renew. Sustain. Energy Rev.* **2016**, *55*, 467–481. [CrossRef]
11. Hasan, M.D.M.; Wang, X.S.; Mourant, D.; Gunawan, R.; Yu, C.; Hu, X.; Kadarwati, S.; Gholizadeh, M.; Wu, H.; Li, B.; et al. Grinding pyrolysis of Mallee wood: Effects of pyrolysis conditions on the yields of bio-oil and biochar. *Fuel Process. Technol.* **2017**, *167*, 215–220. [CrossRef]
12. Sohaib, Q.; Habib, M.; Fawad Ali Shah, S.; Habib, U.; Ullah, S. Fast pyrolysis of locally available green waste at different residence time and temperatures. *Energy Sources Part A Recovery Util. Environ. Eff.* **2017**, *39*, 1639–1646. [CrossRef]
13. Solar, J.; de Marco, I.; Caballero, B.M.; Lopez-Urionabarrenechea, A.; Rodriguez, N.; Agirre, I.; Adrados, A. Influence of temperature and residence time in the pyrolysis of woody biomass waste in a continuous screw reactor. *Biomass Bioenergy* **2016**, *95*, 416–423. [CrossRef]
14. Cuypers, F.; Helsen, L. Pyrolysis of chromated copper arsenate (CCA) treated wood waste at elevated pressure: Influence of particle size, heating rate, residence time, temperature and pressure. *J. Anal. Appl. Pyrolysis* **2011**, *92*, 111–122. [CrossRef]
15. Newalkar, G.; Iisa, K.; D'Amico, A.D.; Sievers, C.; Agrawal, P. Effect of Temperature, Pressure, and Residence Time on Pyrolysis of Pine in an Entrained Flow Reactor. *Energy Fuels* **2014**, *28*, 5144–5157. [CrossRef]
16. Luo, S.; Xiao, B.; Hu, Z.; Liu, S. Effect of particle size on pyrolysis of single-component municipal solid waste in fixed bed reactor. *Int. J. Hydrogen Energy* **2010**, *35*, 93–97. [CrossRef]

17. Yorgun, S.; Yıldız, D. Slow pyrolysis of paulownia wood: Effects of pyrolysis parameters on product yields and bio-oil characterization. *J. Anal. Appl. Pyrolysis* **2015**, *114*, 68–78. [CrossRef]
18. Varma, A.K.; Thakur, L.S.; Shankar, R.; Mondal, P. Pyrolysis of wood sawdust: Effects of process parameters on products yield and characterization of products. *Waste Manag.* **2019**, *89*, 224–235. [CrossRef] [PubMed]
19. Bennadji, H.; Smith, K.; Serapiglia, M.J.; Fisher, E.M. Effect of Particle Size on Low-Temperature Pyrolysis of Woody Biomass. *Energy Fuels* **2014**, *28*, 7527–7537. [CrossRef]
20. Zhang, L.; Li, S.; Li, K.; Zhu, X. Two-step pyrolysis of corncob for value-added chemicals and high quality bio-oil: Effects of pyrolysis temperature and residence time. *Energy Convers. Manag.* **2018**, *166*, 260–267. [CrossRef]
21. Singh, A.; Nanda, S.; Guayaquil-Sosa, J.F.; Berruti, F. Pyrolysis of Miscanthus and characterization of value-added bio-oil and biochar products. *Can. J. Chem. Eng.* **2021**, *99* (Suppl. S1), S55–S68. [CrossRef]
22. Xiong, Z.; Fang, Z.; Jiang, L.; Han, H.; He, L.; Xu, K.; Xu, J.; Su, S.; Hu, S.; Wang, Y.; et al. Comparative study of catalytic and non-catalytic steam reforming of bio-oil: Importance of pyrolysis temperature and its parent biomass particle size during bio-oil production process. *Fuel* **2022**, *314*, 122746. [CrossRef]
23. Charis, G.; Danha, G.; Muzenda, E. Optimizing Yield and Quality of Bio-Oil: A Comparative Study of Acacia tortilis and Pine Dust. *Processes* **2020**, *8*, 551. [CrossRef]
24. *ASTM E871-82*; Standard Test Method for Moisture Analysis of Particulate Wood Fuels. ASTM International: West Conshohocken, PA, USA, 2019.
25. Abitbol, T.; Marway, H.; Cranston, E.D. Surface modification of cellulose nanocrystals with cetyltrimethylammonium bromide. *Nord. Pulp Pap. Res. J.* **2014**, *29*, 46–57. [CrossRef]
26. Hasan, M.M.; Rasul, M.G.; Ashwath, N.; Khan, M.M.K.; Jahirul, M.I. Fast pyrolysis of Beauty Leaf Fruit Husk (BLFH) in an auger reactor: Effect of temperature on the yield and physicochemical properties of BLFH oil. *Renew. Energy* **2022**, *194*, 1098–1109. [CrossRef]
27. Kumar Mishra, R.; Mohanty, K. Kinetic analysis and pyrolysis behavior of low-value waste lignocellulosic biomass for its bioenergy potential using thermogravimetric analyzer. *Mater. Sci. Energy Technol.* **2021**, *4*, 136–147. [CrossRef]
28. Singh, R.K.; Pandey, D.; Patil, T.; Sawarkar, A.N. Pyrolysis of banana leaves biomass: Physico-chemical characterization, thermal decomposition behavior, kinetic and thermodynamic analyses. *Bioresour. Technol.* **2020**, *310*, 123464. [CrossRef] [PubMed]
29. Mumbach, G.D.; Alves, J.L.F.; da Silva, J.C.G.; Domenico, M.D.; Arias, S.; Pacheco, J.G.A.; Marangoni, C.; Machado, R.A.F.; Bolzan, A. Prospecting pecan nutshell pyrolysis as a source of bioenergy and bio-based chemicals using multicomponent kinetic modeling, thermodynamic parameters estimation, and Py-GC/MS analysis. *Renew. Sustain. Energy Rev.* **2022**, *153*, 111753. [CrossRef]
30. Abu Bakar, M.S.; Ahmed, A.; Jeffery, D.M.; Hidayat, S.; Sukri, R.S.; Mahlia, T.M.I.; Jamil, F.; Khurrum, M.S.; Inayat, A.; Moogi, S.; et al. Pyrolysis of solid waste residues from *Lemon Myrtle* essential oils extraction for bio-oil production. *Bioresour. Technol.* **2020**, *318*, 123913. [CrossRef]
31. Hla, S.S.; Roberts, D. Characterisation of chemical composition and energy content of green waste and municipal solid waste from Greater Brisbane, Australia. *Waste Manag.* **2015**, *41*, 12–19. [CrossRef]
32. Taib, R.M.; Abdullah, N.; Aziz, N.S.M. Bio-oil derived from banana pseudo-stem via fast pyrolysis process. *Biomass Bioenergy* **2021**, *148*, 106034. [CrossRef]
33. Shahbaz, M.; AlNouss, A.; Parthasarathy, P.; Abdelaal, A.H.; Mackey, H.; McKay, G.; Al-Ansari, T. Investigation of biomass components on the slow pyrolysis products yield using Aspen Plus for techno-economic analysis. *Biomass Convers. Biorefinery* **2022**, *12*, 669–681. [CrossRef]
34. Smith, A.M.; Singh, S.; Ross, A.B. Fate of inorganic material during hydrothermal carbonisation of biomass: Influence of feedstock on combustion behaviour of hydrochar. *Fuel* **2016**, *169*, 135–145. [CrossRef]
35. Mettler, M.S.; Vlachos, D.G.; Dauenhauer, P.J. Top ten fundamental challenges of biomass pyrolysis for biofuels. *Energy Environ. Sci.* **2012**, *5*, 7797–7809. [CrossRef]
36. Mabrouki, J.; Abbassi, M.A.; Guedri, K.; Omri, A.; Jeguirim, M. Simulation of biofuel production via fast pyrolysis of palm oil residues. *Fuel* **2015**, *159*, 819–827. [CrossRef]
37. Tsai, W.T.; Lee, M.K.; Chang, Y.M. Fast pyrolysis of rice husk: Product yields and compositions. *Bioresour. Technol.* **2007**, *98*, 22–28. [CrossRef] [PubMed]
38. Perkins, G.; Bhaskar, T.; Konarova, M. Process development status of fast pyrolysis technologies for the manufacture of renewable transport fuels from biomass. *Renew. Sustain. Energy Rev.* **2018**, *90*, 292–315. [CrossRef]
39. Ogunsina, B.; Ojolo, S.; Ohunakin, O.; Oyedeji, O.; Matanmi, K.; Bamgboye, I. Potentials for generating alternative fuels from empty palm fruit bunches by pyrolysis. *Proc. ICCEM* **2012**, *159*, 185–190.
40. Chen, Y.; Liang, S.; Xiao, K.; Hu, J.; Hou, H.; Liu, B.; Deng, H.; Yang, J. A cost-effective strategy for metal recovery from waste printed circuit boards via crushing pretreatment combined with pyrolysis: Effects of particle size and pyrolysis temperature. *J. Clean. Prod.* **2021**, *280*, 124505. [CrossRef]
41. Martínez-Narro, G.; Hassan, S.; Phan, A.N. Chemical recycling of plastic waste for sustainable polymer manufacturing–A critical review. *J. Environ. Chem. Eng.* **2024**, *12*, 112323. [CrossRef]
42. Mani, T.; Murugan, P.; Abedi, J.; Mahinpey, N. Pyrolysis of wheat straw in a thermogravimetric analyzer: Effect of particle size and heating rate on devolatilization and estimation of global kinetics. *Chem. Eng. Res. Des.* **2010**, *88*, 952–958. [CrossRef]

43. Shen, J.; Wang, X.-S.; Garcia-Perez, M.; Mourant, D.; Rhodes, M.J.; Li, C.-Z. Effects of particle size on the fast pyrolysis of oil mallee woody biomass. *Fuel* **2009**, *88*, 1810–1817. [CrossRef]
44. Yu, J.; Sun, L.; Berrueco, C.; Fidalgo, B.; Paterson, N.; Millan, M. Influence of temperature and particle size on structural characteristics of chars from Beechwood pyrolysis. *J. Anal. Appl. Pyrolysis* **2018**, *130*, 127–134. [CrossRef]
45. Arnold, S.; Rodriguez-Uribe, A.; Misra, M.; Mohanty, A.K. Slow pyrolysis of bio-oil and studies on chemical and physical properties of the resulting new bio-carbon. *J. Clean. Prod.* **2018**, *172*, 2748–2758. [CrossRef]
46. Mandal, S.; Bhattacharya, T.K.; Verma, A.K.; Haydary, J. Optimization of process parameters for bio-oil synthesis from pine needles (*Pinus roxburghii*) using response surface methodology. *Chem. Pap.* **2018**, *72*, 603–616. [CrossRef]
47. Gupta, G.K.; Mondal, M.K. Bio-energy generation from sagwan sawdust via pyrolysis: Product distributions, characterizations and optimization using response surface methodology. *Energy* **2019**, *170*, 423–437. [CrossRef]
48. Wądrzyk, M.; Janus, R.; Vos, M.P.; Brilman, D.W.F. Effect of process conditions on bio-oil obtained through continuous hydrothermal liquefaction of Scenedesmus sp. microalgae. *J. Anal. Appl. Pyrolysis* **2018**, *134*, 415–426. [CrossRef]
49. Singh, S.; Chakraborty, J.P.; Mondal, M.K. Pyrolysis of torrefied biomass: Optimization of process parameters using response surface methodology, characterization, and comparison of properties of pyrolysis oil from raw biomass. *J. Clean. Prod.* **2020**, *272*, 122517. [CrossRef]
50. Daimary, N.; Boruah, P.; Eldiehy, K.S.H.; Pegu, T.; Bardhan, P.; Bora, U.; Mandal, M.; Deka, D. Musa acuminata peel: A bioresource for bio-oil and by-product utilization as a sustainable source of renewable green catalyst for biodiesel production. *Renew. Energy* **2022**, *187*, 450–462. [CrossRef]
51. Daimary, N.; Eldiehy, K.S.H.; Boruah, P.; Deka, D.; Bora, U.; Kakati, B.K. Potato peels as a sustainable source for biochar, bio-oil and a green heterogeneous catalyst for biodiesel production. *J. Environ. Chem. Eng.* **2022**, *10*, 107108. [CrossRef]
52. Sowmya Dhanalakshmi, C.; Madhu, P. Utilization possibilities of Albizia amara as a source of biomass energy for bio-oil in pyrolysis process. *Energy Sources Part A Recovery Util. Environ. Eff.* **2019**, *41*, 1908–1919. [CrossRef]
53. Ren, S.; Ye, X.P. Stability of crude bio-oil and its water-extracted fractions. *J. Anal. Appl. Pyrolysis* **2018**, *132*, 151–162. [CrossRef]
54. Kumar, R.; Strezov, V.; Lovell, E.; Kan, T.; Weldekidan, H.; He, J.; Dastjerdi, B.; Scott, J. Bio-oil upgrading with catalytic pyrolysis of biomass using Copper/zeolite-Nickel/zeolite and Copper-Nickel/zeolite catalysts. *Bioresour. Technol.* **2019**, *279*, 404–409. [CrossRef]
55. Isa, K.M.; Daud, S.; Hamidin, N.; Ismail, K.; Saad, S.A.; Kasim, F.H. Thermogravimetric analysis and the optimisation of bio-oil yield from fixed-bed pyrolysis of rice husk using response surface methodology (RSM). *Ind. Crops Prod.* **2011**, *33*, 481–487. [CrossRef]
56. Hilten, R.N.; Speir, R.A.; Kastner, J.R.; Mani, S.; Das, K.C. Effect of Torrefaction on Bio-oil Upgrading over HZSM-5. Part 1: Product Yield, Product Quality, and Catalyst Effectiveness for Benzene, Toluene, Ethylbenzene, and Xylene Production. *Energy Fuels* **2013**, *27*, 830–843. [CrossRef]
57. Machado, H.; Cristino, A.F.; Orišková, S.; Galhano dos Santos, R. Bio-Oil: The Next-Generation Source of Chemicals. *Reactions* **2022**, *3*, 118–137. [CrossRef]
58. Quraishi, M.A.; Chauhan, D.S.; Ansari, F.A. Development of environmentally benign corrosion inhibitors for organic acid environments for oil-gas industry. *J. Mol. Liq.* **2021**, *329*, 115514. [CrossRef]
59. Kabbour, M.; Luque, R. Chapter 10—Furfural as a Platform Chemical: From Production to Applications. In *Biomass, Biofuels, Biochemicals*; Saravanamurugan, S., Pandey, A., Li, H., Riisager, A., Eds.; Elsevier: Amsterdam, The Netherlands, 2020; pp. 283–297.
60. Yang, H.; de Wild, P.; Lahive, C.W.; Wang, Z.; Deuss, P.J.; Heeres, H.J. Experimental studies on a combined pyrolysis/staged condensation/hydrotreatment approach to obtain biofuels and biobased chemicals. *Fuel Process. Technol.* **2022**, *228*, 107160. [CrossRef]
61. Ahmad, R.; Hamidin, N.; Ali, U.; Abidin, C. Characterization of bio-oil from palm kernel shell pyrolysis. *J. Mech. Eng. Sci.* **2014**, *7*, 1134–1140. [CrossRef]
62. Williams, P.T.; Horne, P.A. Analysis of aromatic hydrocarbons in pyrolytic oil derived from biomass. *J. Anal. Appl. Pyrolysis* **1995**, *31*, 15–37. [CrossRef]
63. Zhang, Q.; Chang, J.; Wang, T.; Xu, Y. Review of biomass pyrolysis oil properties and upgrading research. *Energy Convers. Manag.* **2007**, *48*, 87–92. [CrossRef]
64. Thring, R.W.; Katikaneni, S.P.R.; Bakhshi, N.N. The production of gasoline range hydrocarbons from Alcell® lignin using HZSM-5 catalyst. *Fuel Process. Technol.* **2000**, *62*, 17–30. [CrossRef]
65. Wang, S.; Zhao, S.; Uzoejinwa, B.B.; Zheng, A.; Wang, Q.; Huang, J.; Abomohra, A.E.-F. A state-of-the-art review on dual purpose seaweeds utilization for wastewater treatment and crude bio-oil production. *Energy Convers. Manag.* **2020**, *222*, 113253. [CrossRef]
66. Salehi, E.; Abedi, J.; Harding, T. Bio-oil from Sawdust: Effect of Operating Parameters on the Yield and Quality of Pyrolysis Products. *Energy Fuels* **2011**, *25*, 4145–4154. [CrossRef]
67. Wang, C.; Luo, Z.; Li, S.; Zhu, X. Coupling effect of condensing temperature and residence time on bio-oil component enrichment during the condensation of biomass pyrolysis vapors. *Fuel* **2020**, *274*, 117861. [CrossRef]
68. Liu, s.; Zhao, H.; Fan, T.; Zhou, J.; Liu, X.; Li, Y.; Zhao, G.; Wang, Y.; Zeng, M. Investigation on chemical structure and hydrocarbon generation potential of lignite in the different pretreatment process. *Fuel* **2021**, *291*, 120205. [CrossRef]

69. Qureshi, K.M.; Kay Lup, A.N.; Khan, S.; Abnisa, F.; Wan Daud, W.M.A. Optimization of palm shell pyrolysis parameters in helical screw fluidized bed reactor: Effect of particle size, pyrolysis time and vapor residence time. *Clean. Eng. Technol.* **2021**, *4*, 100174. [CrossRef]
70. Zhou, X.; Moghaddam, T.B.; Chen, M.; Wu, S.; Zhang, Y.; Zhang, X.; Adhikari, S.; Zhang, X. Effects of pyrolysis parameters on physicochemical properties of biochar and bio-oil and application in asphalt. *Sci. Total Environ.* **2021**, *780*, 146448. [CrossRef]
71. DeSisto, W.J.; Hill, N.; Beis, S.H.; Mukkamala, S.; Joseph, J.; Baker, C.; Ong, T.-H.; Stemmler, E.A.; Wheeler, M.C.; Frederick, B.G.; et al. Fast Pyrolysis of Pine Sawdust in a Fluidized-Bed Reactor. *Energy Fuels* **2010**, *24*, 2642–2651. [CrossRef]
72. Abdullahi, N.; Sulaiman, F.; Safana, A.A. Bio-oil and biochar derived from the pyrolysis of palm kernel shell for briquette. *Sains Malays.* **2017**, *46*, 2441–2445. [CrossRef]
73. Iáñez-Rodríguez, I.; Martín-Lara, M.A.; Blázquez, G.; Calero, M. Effect of different pre-treatments and addition of plastic on the properties of bio-oil obtained by pyrolysis of greenhouse crop residue. *J. Anal. Appl. Pyrolysis* **2021**, *153*, 104977. [CrossRef]
74. Kumar, R.; Strezov, V.; Weldekidan, H.; He, J.; Singh, S.; Kan, T.; Dastjerdi, B. Lignocellulose biomass pyrolysis for bio-oil production: A review of biomass pre-treatment methods for production of drop-in fuels. *Renew. Sustain. Energy Rev.* **2020**, *123*, 109763. [CrossRef]
75. Dhyani, V.; Bhaskar, T. A comprehensive review on the pyrolysis of lignocellulosic biomass. *Renew. Energy* **2018**, *129*, 695–716. [CrossRef]
76. Onay, O. Influence of pyrolysis temperature and heating rate on the production of bio-oil and char from safflower seed by pyrolysis, using a well-swept fixed-bed reactor. *Fuel Process. Technol.* **2007**, *88*, 523–531. [CrossRef]
77. Ahmed, A.; Abu Bakar, M.S.; Sukri, R.S.; Hussain, M.; Farooq, A.; Moogi, S.; Park, Y.-K. Sawdust pyrolysis from the furniture industry in an auger pyrolysis reactor system for biochar and bio-oil production. *Energy Convers. Manag.* **2020**, *226*, 113502. [CrossRef]
78. Ahmed, A.; Abu Bakar, M.S.; Azad, A.K.; Sukri, R.S.; Phusunti, N. Intermediate pyrolysis of Acacia cincinnata and Acacia holosericea species for bio-oil and biochar production. *Energy Convers. Manag.* **2018**, *176*, 393–408. [CrossRef]
79. Park, J.Y.; Kim, J.-K.; Oh, C.-H.; Park, J.-W.; Kwon, E.E. Production of bio-oil from fast pyrolysis of biomass using a pilot-scale circulating fluidized bed reactor and its characterization. *J. Environ. Manag.* **2019**, *234*, 138–144. [CrossRef]
80. Budarin, V.L.; Clark, J.H.; Lanigan, B.A.; Shuttleworth, P.; Breeden, S.W.; Wilson, A.J.; Macquarrie, D.J.; Milkowski, K.; Jones, J.; Bridgeman, T.; et al. The preparation of high-grade bio-oils through the controlled, low temperature microwave activation of wheat straw. *Bioresour. Technol.* **2009**, *100*, 6064–6068. [CrossRef]
81. Cai, W.; Liu, R.; He, Y.; Chai, M.; Cai, J. Bio-oil production from fast pyrolysis of rice husk in a commercial-scale plant with a downdraft circulating fluidized bed reactor. *Fuel Process. Technol.* **2018**, *171*, 308–317. [CrossRef]
82. Neumann, J.; Binder, S.; Apfelbacher, A.; Gasson, J.R.; Ramírez García, P.; Hornung, A. Production and characterization of a new quality pyrolysis oil, char and syngas from digestate—Introducing the thermo-catalytic reforming process. *J. Anal. Appl. Pyrolysis* **2015**, *113*, 137–142. [CrossRef]
83. Kontoulis, P.; Kazangas, D.; Doss, T.P.; Kaiktsis, L. Development and CFD Validation of an Integrated Model for Marine Heavy Fuel Oil Thermophysical Properties. *J. Energy Eng.* **2018**, *144*, 04018059. [CrossRef]
84. Shafaghat, H.; Kim, J.M.; Lee, I.-G.; Jae, J.; Jung, S.-C.; Park, Y.-K. Catalytic hydrodeoxygenation of crude bio-oil in supercritical methanol using supported nickel catalysts. *Renew. Energy* **2019**, *144*, 159–166. [CrossRef]
85. Ibarra, Á.; Hita, I.; Arandes, J.M.; Bilbao, J. Influence of the Composition of Raw Bio-Oils on Their Valorization in Fluid Catalytic Cracking Conditions. *Energy Fuels* **2019**, *33*, 7458–7465. [CrossRef]
86. de Castro, D.A.R.; da Silva Ribeiro, H.J.; Ferreira, C.C.; de Andrade Cordeiro, M.; Guerreiro, L.H.H.; Pereira, A.M.; dos Santos, W.; Santos, M.C.; de Carvalho, F.B.; Jose, O.C.S., Jr. Fractional Distillation of Bio-Oil Produced by Pyrolysis of Açaí (Euterpe oleracea) Seeds. In *Fractionation*; InTechOpen: London, UK, 2019; p. 61.
87. Sondakh, R.C.; Hambali, E.; Indrasti, N.S. Improving characteristic of bio-oil by esterification method. *IOP Conf. Ser. Earth Environ. Sci.* **2019**, *230*, 012071. [CrossRef]
88. Jiang, X.; Ellis, N. Upgrading Bio-oil through Emulsification with Biodiesel: Mixture Production. *Energy Fuels* **2010**, *24*, 1358–1364. [CrossRef]